

Supplementary Materials for

**Mechanistic basis of choline import involved in teichoic acids and  
lipopolysaccharide modification**

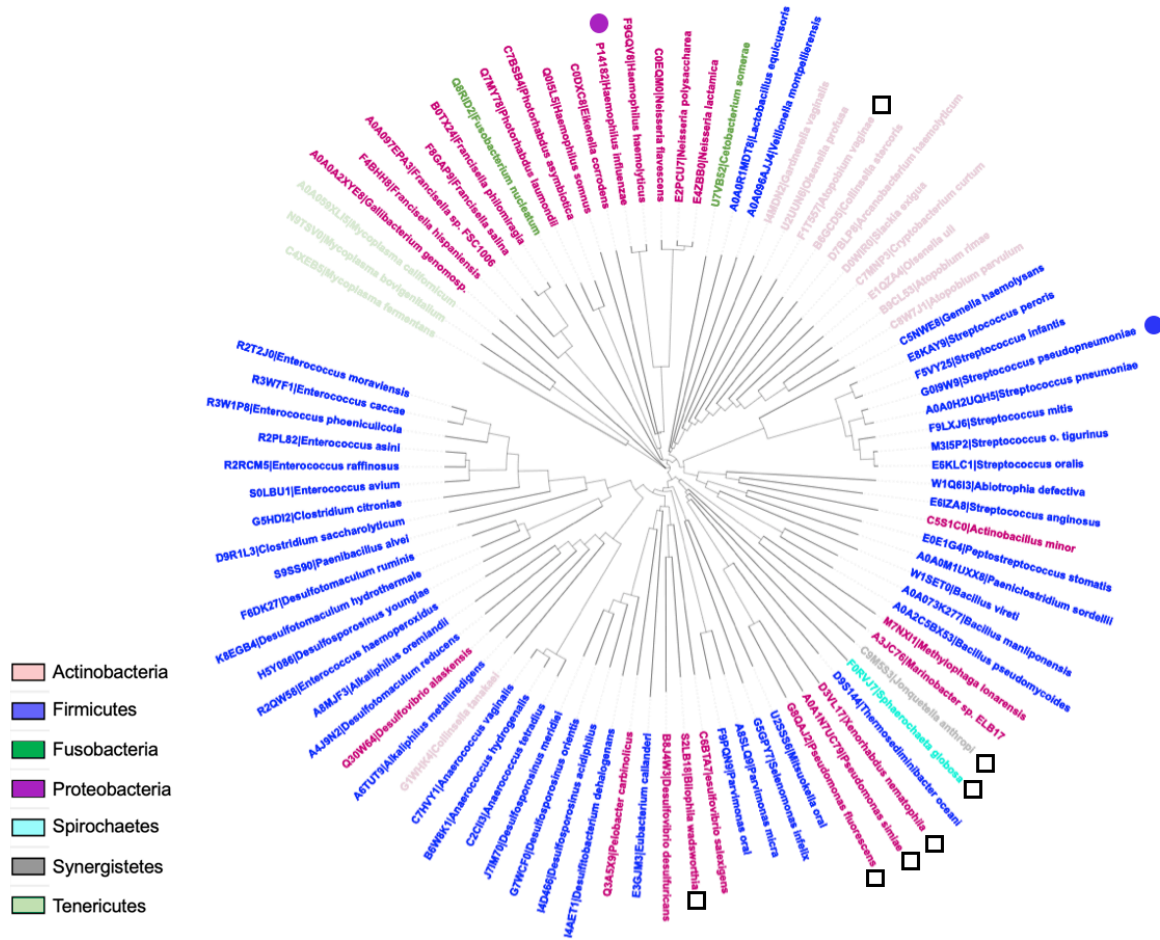
Natalie Bärlund, Anne-Stéphanie Rueff, Gonzalo Cebrero, Cedric A. J. Hutter,  
Markus A. Seeger, Jan-Willem Veening, Camilo Perez\*

\*Corresponding author. Email: camilo.perez@unibas.ch

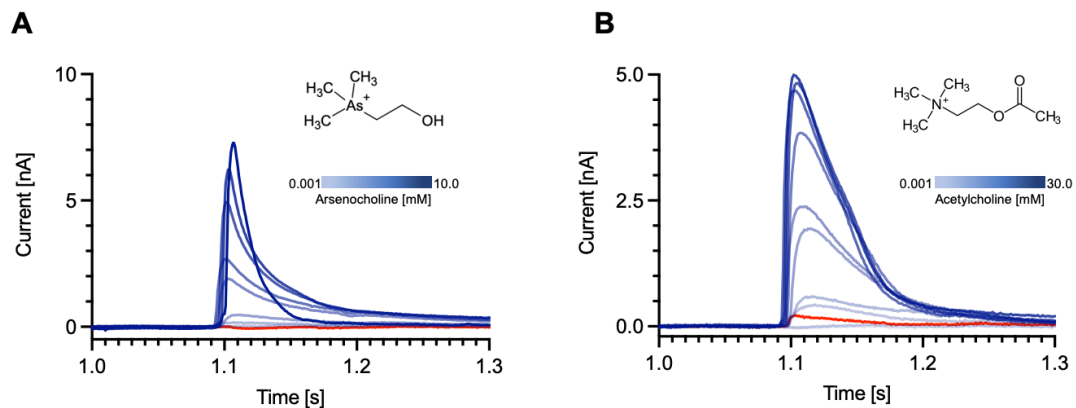
Published 2 March 2022, *Sci. Adv.* **8**, eabm1122 (2022)  
DOI: 10.1126/sciadv.abm1122

**This PDF file includes:**

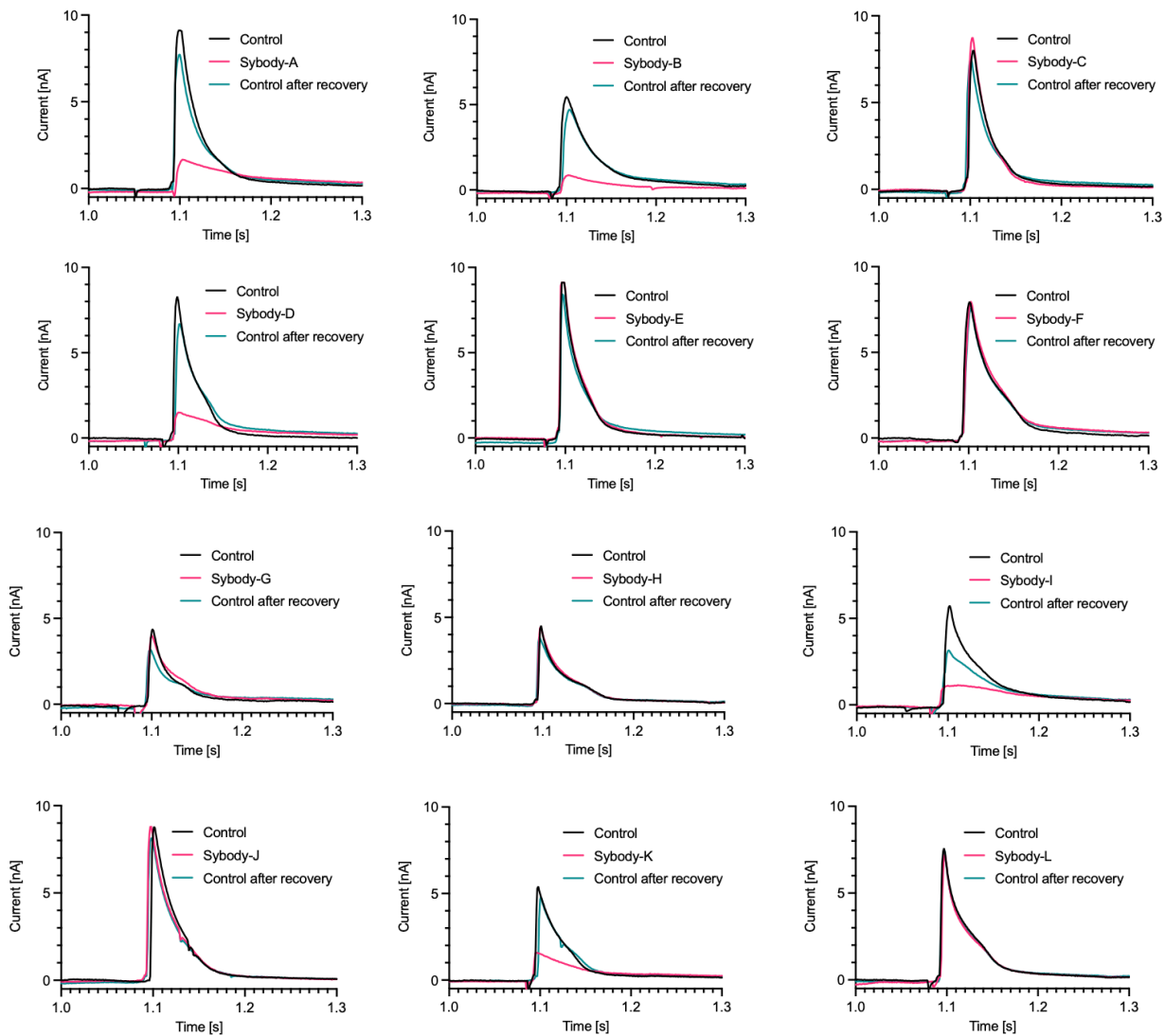
Supplementary Text  
Figs. S1 to S13  
Table S1



**Fig. S1. LicB is conserved across divergent bacteria phyla.** Phylogenetic tree of bacteria species across multiple phyla where *lic* operon genes involved in choline uptake (*licB*) and activation (*licA* and *licC*) are conserved. Phyla are depicted by colors according to the inset. *S. pneumoniae* and *H. influenzae* are indicated by blue and magenta dots. White squares show bacteria species where residues E170 and R191 are not conserved (see Fig. 4).

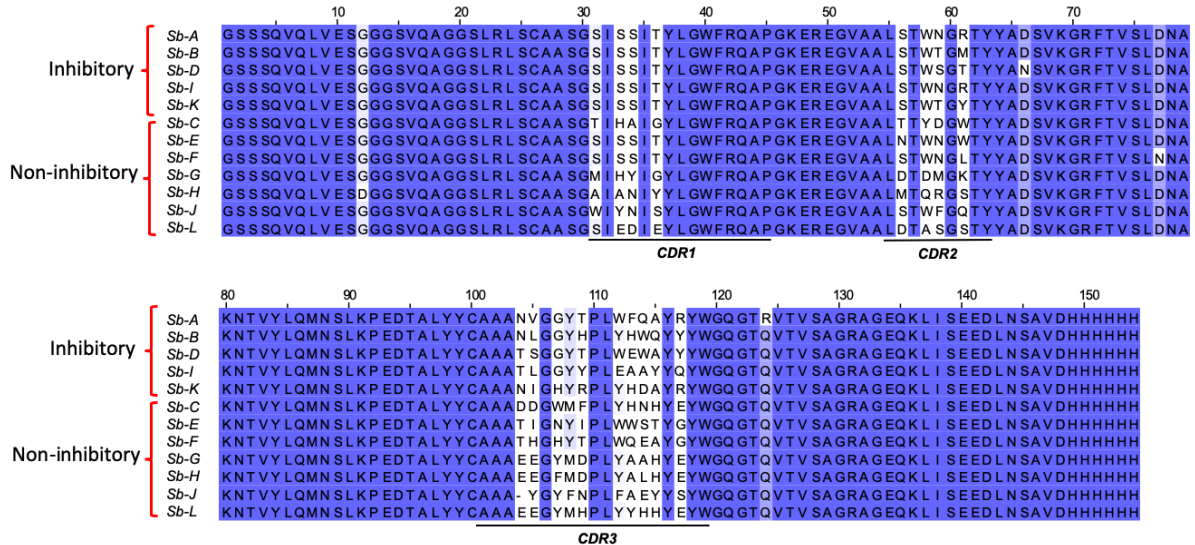


**Fig. S2. LicB displays promiscuous selectivity towards arsenocholine and acetylcholine.** SSM-electrophysiology recordings of currents measured during application of arsenocholine (**A**) or acetylcholine (**B**) are indicated by blue curves. Protein-free liposomes traces measured in presence of 5 mM arsenocholine (**A**) or 30 mM acetylcholine (**B**) are shown in red. The amplitude of the peak currents was used for determination of EC<sub>50</sub> values as shown in Fig. 2B.

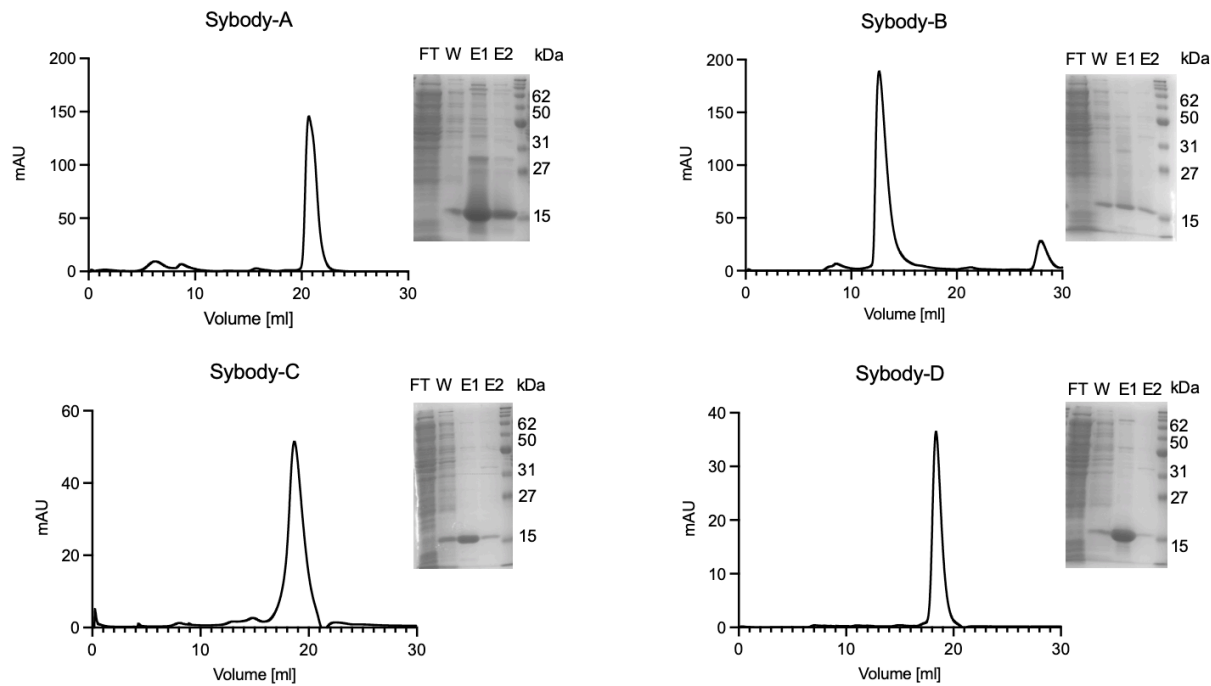


**Fig. S3. SSM-electrophysiology recordings of LicB choline transport in presence of sybodies.**

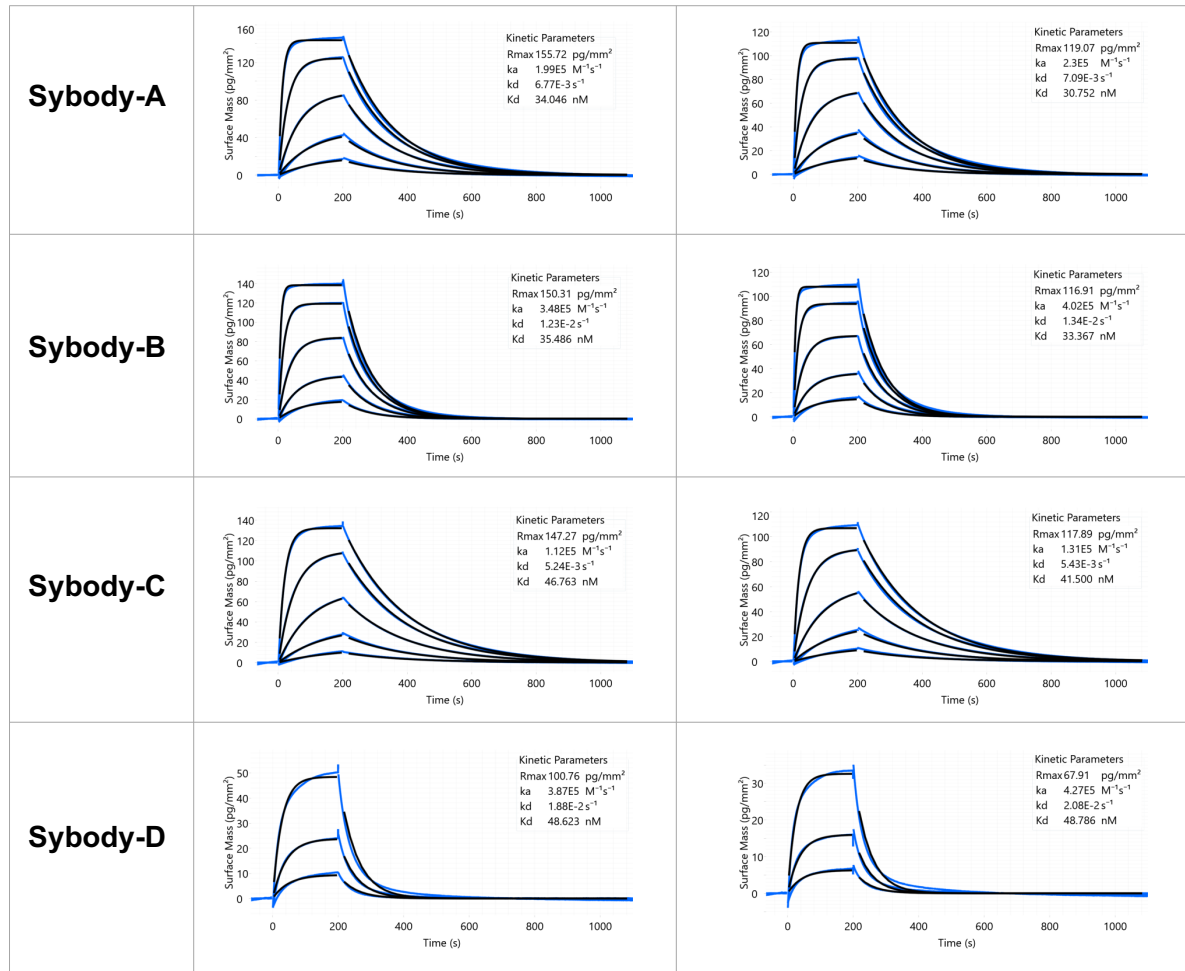
Representative recordings of currents measured during application of 5 mM choline in absence of sybodies are shown in black (control). The same experiment but in presence of 500 nM of sybodies are shown in pink, whereas recordings after unbinding of sybodies are shown in green. The amplitudes of the peak currents (pink traces) were used for the generation of the histogram shown in Fig. 2D.



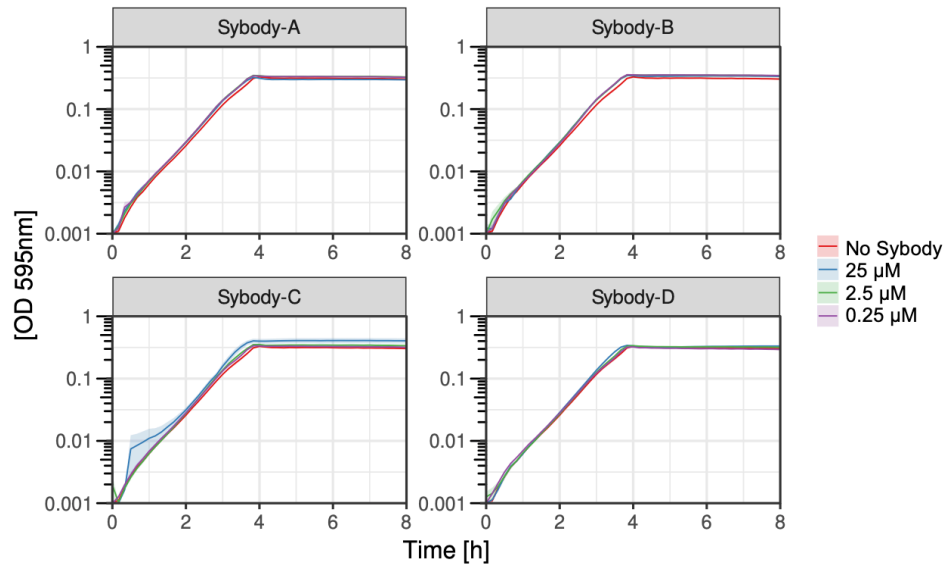
**Fig. S4. Sequence conservation alignment of sybodies characterized by SSM-electrophysiology.** Inhibitory and non-inhibitory sybodies are grouped together. CDR Regions are indicated. All sybodies belong to the convex library displaying a long CDR3 region.



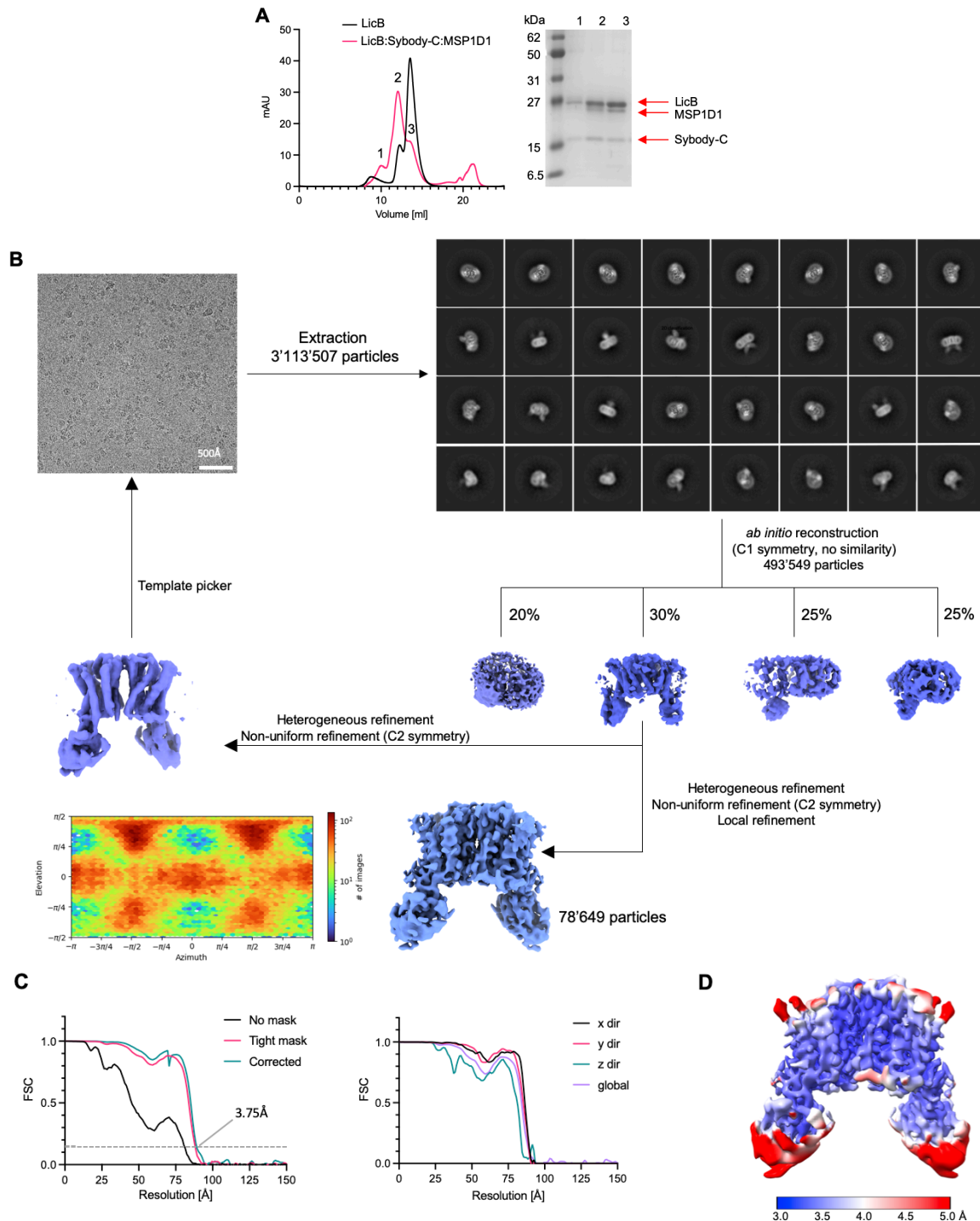
**Fig. S5. Purification of sybodies A, B, C and D.** (*Left*) Size exclusion profiles using a Superdex 200 Increase 10/300 column. (*Right*) SDS-PAGE of samples from different steps of sybodies purification. FT, flow through. W, washing of column. E1 and E2, two steps elution.



**Fig. S6. Determination of binding affinity of Sybodies to LicB by grating-coupled interferometry (GCI).** The four sybodies were injected at 5, 15, 45, 135 and 405 nM concentrations in absence (*left*) or presence of 5 mM choline (*right*). Data are shown in blue and fitting curves in black. Data were fitted using a Langmuir 1:1 model.

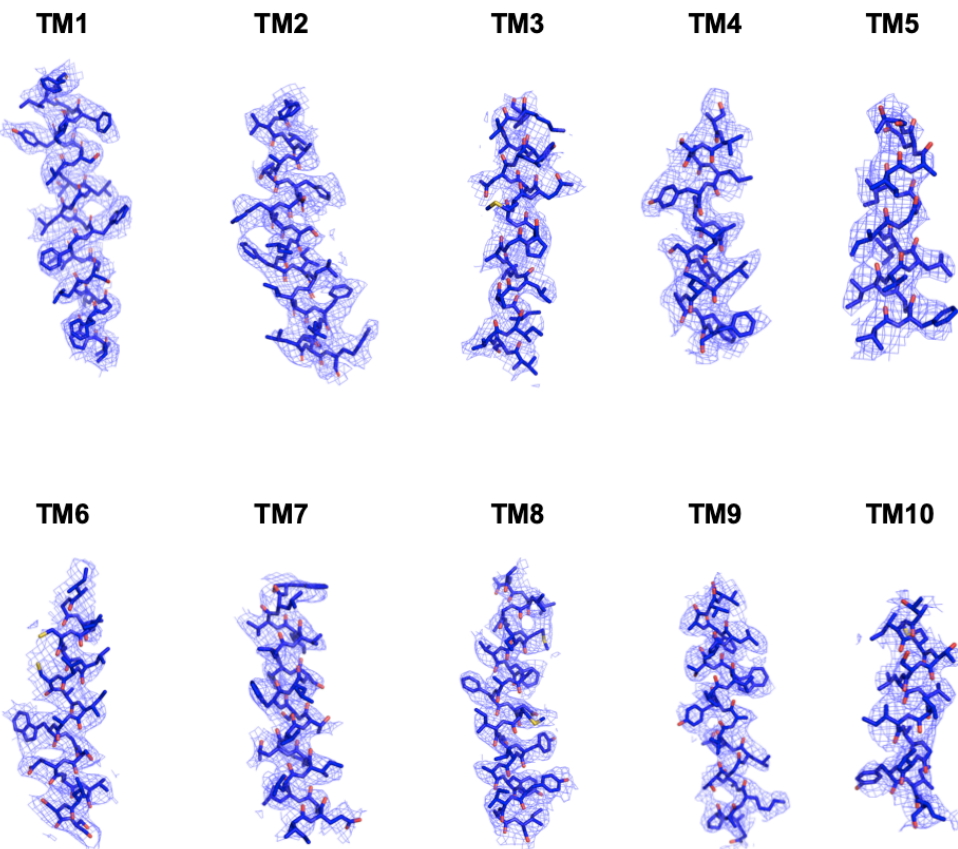
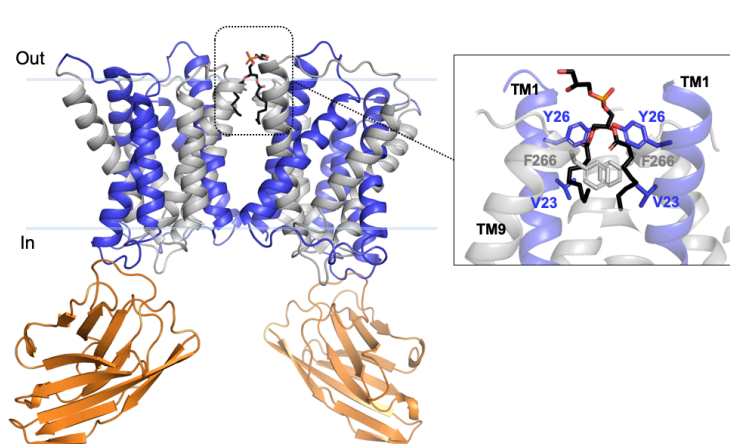
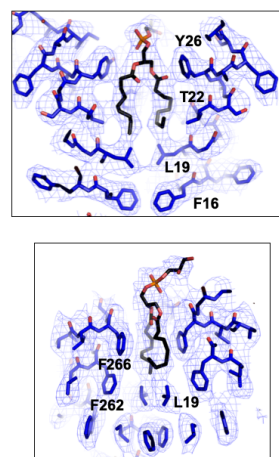


**Fig. S7. *S. pneumoniae* growth in presence of sybodies.** Growth curves of unencapsulated *S. pneumoniae* in presence of sybodies targeting LicB in C+Y media supplemented with choline. Three different concentrations of sybodies were tested in comparison with growth without sybody. An average of three replicates and standard error of the mean are plotted.



**Fig. S8. Cryo-EM reconstruction of LicB-Sybody-C complex in lipid nanodiscs.** **A.** Size exclusion chromatography profiles of LicB and LicB:Sybody-C complex reconstituted in nanodiscs in a Superdex 200 Increase 10/300 column. SDS-PAGE of the three main peaks of the red trace is shown. **B.** Representative micrograph of the complex acquired with a Glacios TEM equipped with a K3 camera. The data processing workflow shows 2D classes of LicB:Sybody-C:MSP1D1 after particle extraction and multiple rounds of 2D classification and *ab initio* reconstruction. **C.** FSC curves for resolution analysis. **D.** 3D density map of the LicB-Sybody-C complex.

reconstruction performed with four classes. The particle classes with best protein-like features were used for further rounds of 3D classification, non-uniform refinement, and template generation. The selected particles were later used for a new round of particle picking. Further processing led to a new optimized set of particles used as an input for iterative heterogeneous, non-uniform, and local refinement rounds with C<sub>2</sub>-symmetry, which yielded a map at a resolution of 3.75 Å. The heatmap displays the number of particles for a given viewing angle. **C.** (*Left*) FSC plots of masked and unmasked maps calculated by cryoSPARC v.3.2.0. The dashed line indicates a 0.143 cut-off. (*Right*) Directional and global FSC plots calculated by the 3DFSC server. The directional FSC curves providing an estimation of anisotropy of the dataset are shown for directions x, y, and z. **D.** Final 3D reconstruction of the LicB:Sybody-C complex colored according to the local resolution, estimated in cryoSPARC v.3.2.0.

**A****B****C**

**Fig. S9. Cryo-EM densities of LicB segments.** **A.** Sections of the cryo-EM density superimposed on the refined structure of LicB. **B.** Side view of the LicB homodimer and bound Sybodies. Inverted repeats TM1-5 and TM6-10 in blue and grey, respectively. Sybody-C is shown in orange. The inset shows a putative POPG lipid molecule present at the dimer interface between both protomers. Surrounding residues are shown and the helices denoted. **C.** Cryo-EM density (mesh) superimposed on the POPG lipid and surrounding residues.

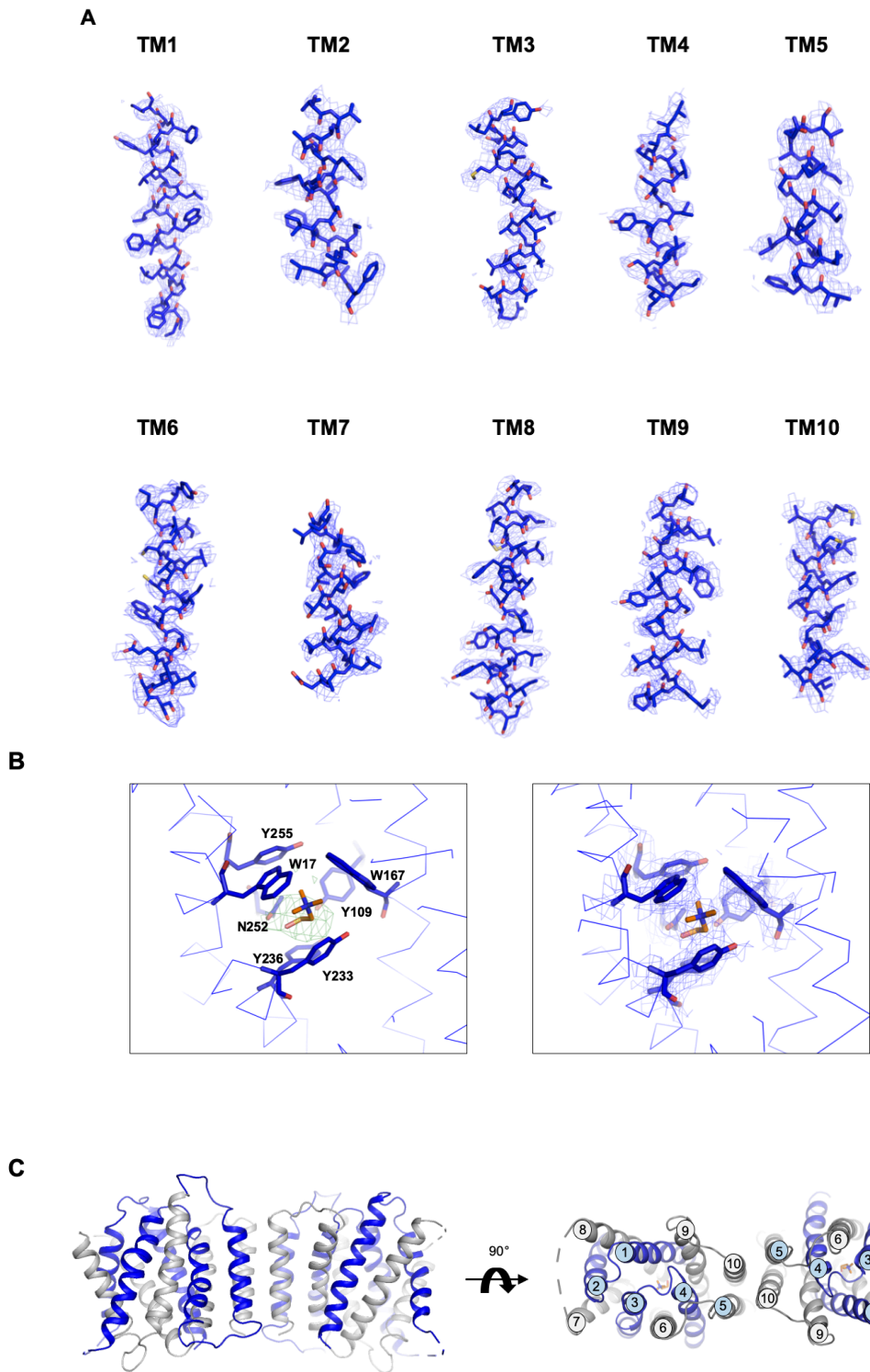


**Fig. S10. Crystal structure of LicB.** **A.**  $2Fo-Fc$  electron density map of individual TM segments of LicB at 1.0  $\sigma$  level. **B.** (Left)  $Fo-Fc$  map at 3.0  $\sigma$  level showing a positive peak at the central binding site before placing choline in the model and refinement. (Right)  $2Fo-Fc$  electron density map of choline and coordinating residues after refinement. **C.** Packing of two LicB molecules in the crystal lattice, resembling the arrangement of dimers in other DMT transporters.

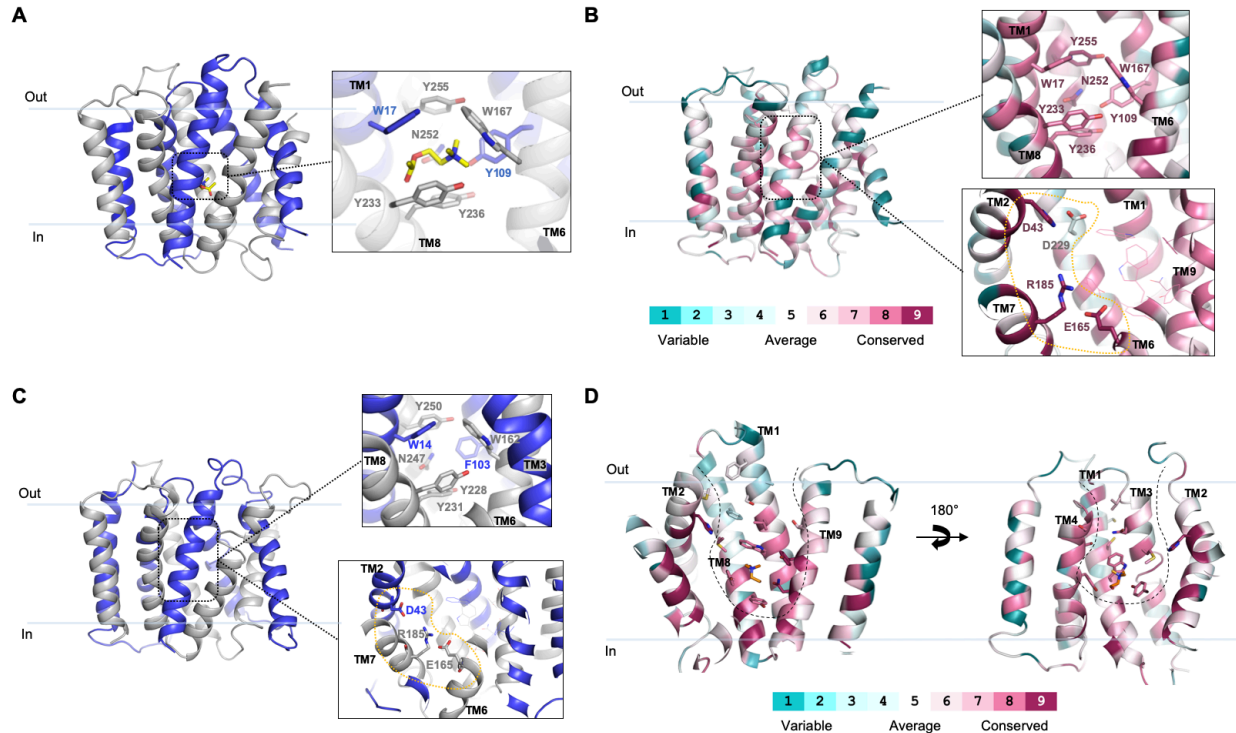


**Figure S11. Docking of acetylcholine and conservation analysis of residues at the choline binding pocket and surrounding charged residues.** **A.** Docking of acetylcholine in LicB central cavity. Acetylcholine is shown in yellow. (Right) Surrounding residues. **B.** Sequence conservation analysis. A multiple sequence alignment of LicB homologues sharing more than 35% identity was generated and residues in the LicB structure were colored by sequence conservation (ConSurf server). (Top right) Residues at the Choline binding site. (Bottom right) Charged residues close to the choline binding site. **C.** Homology model of *H. influenzae* LicB. (Top right) Residues at the Choline binding. (Bottom right) Charged residues close to the choline binding site. **D.** Sequence conservation analysis as in B. showing a slice through the binding cavity from two sides. Conservation and variability are colored according to the legend shown below. Choline is shown in orange. The access to the cavity from the extracellular side is depicted with dotted lines.

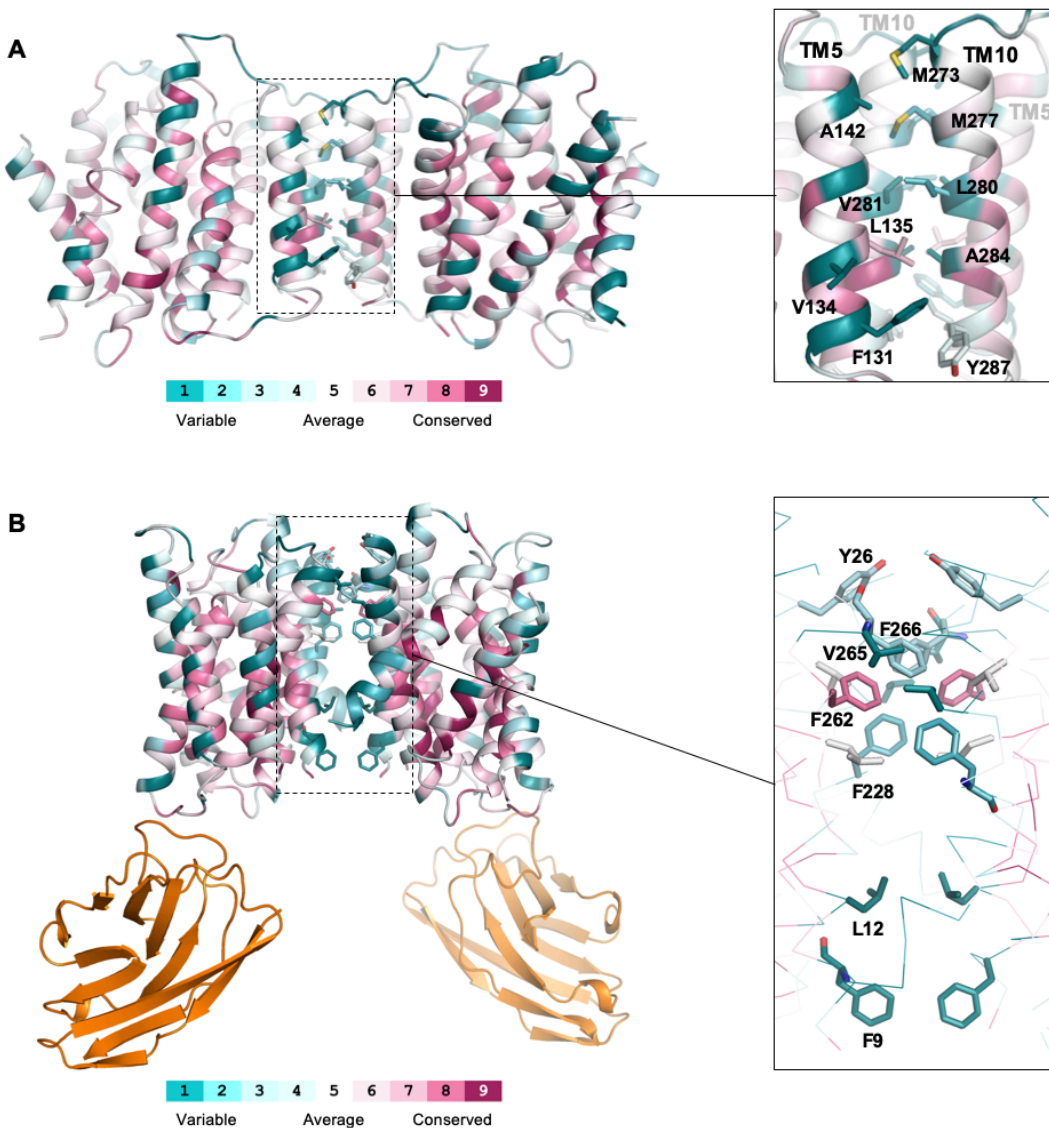
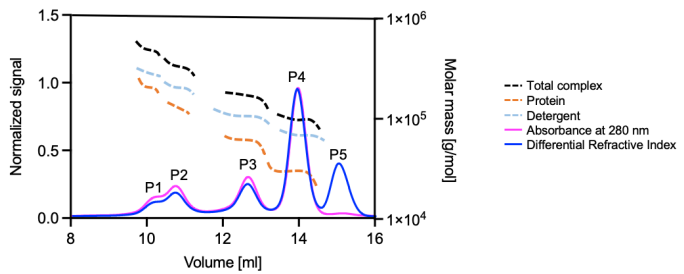


**Figure S12. Conservation analysis of residues at the dimer interface.** **A.** LicB symmetry partners from the crystal structure. The residues in the LicB dimers are colored according to the sequence conservation from a multiple sequence alignment of LicB homologues sharing more than 35% identity (ConSurf server). (*Right*) Residues at the interface of the symmetry partner. **B.** Cryo-EM solved structure of LicB as a dimer in nanodiscs. The residues are colored according to the conservation as in A. (*Right*) Residues at the dimer interface.



Peak	Molecular weight [kDa]			Interpretation
	Total	Detergent	Protein	
P1	561	329	232	Hexamer
P2	421	257	164	Tetramer
P3	206	131	75	Dimer
P4	125	88	37	Monomer
P5	67	66	1	Empty micelles

**Fig. S13. Size exclusion chromatography with multi-angle light scattering (SEC-MALS) analysis of purified LicB in detergent micelles.** Size exclusion profile is plotted as normalized signal and MALS apparent molecular masses of the protein in buffer, detergent in buffer and the total complex with dotted lines (right axis). The molecular weights are summarized in the table with the apparent masses of empty micelles (P5), the monomer (P4, main population), dimer (P3), tetramer (P2) and hexamer (P1).

**Table S1.**

Oligos used in this study.

Strain	Genotype	Reference
D39V	WT strain of clinical isolate, Serotype 2, parent strain for all strains used in this study unless described	Domenech et al., 2018
VL333	<i>prsI::PF6-lacI-tetR</i> ( <i>gen</i> )	Sorg et al., 2020
VL1998	<i>prsI::PF6-lacI</i> ( <i>gen</i> ), <i>bgaA::Plac-dCas9sp</i> ( <i>tet</i> )	Liu et al., 2017
VL4243	<i>prsI::PF6-lacI-tetR</i> ( <i>gen</i> ), <i>bgaA::Plac-licB</i> ( <i>tet</i> )	This study
VL4249	<i>prsI::PF6-lacI-tetR</i> ( <i>gen</i> ), <i>bgaA::Plac-licB</i> ( <i>tet</i> ), <i>zip::Ptet-licB</i> ( <i>spc</i> ), <i>licB::ery</i>	Veening collection
VL4250	<i>prsI::PF6-lacI-tetR</i> ( <i>gen</i> ), <i>bgaA::Plac-licB-Y233A</i> ( <i>tet</i> )	This study
VL4251	<i>prsI::PF6-lacI-tetR</i> ( <i>gen</i> ), <i>bgaA::Plac-licB-Y236A</i> ( <i>tet</i> )	This study
VL4252	<i>prsI::PF6-lacI-tetR</i> ( <i>gen</i> ), <i>bgaA::Plac-licB-W17A</i> ( <i>tet</i> )	This study
VL4253	<i>prsI::PF6-lacI-tetR</i> ( <i>gen</i> ), <i>bgaA::Plac-licB-W167A</i> ( <i>tet</i> )	This study
VL4254	<i>prsI::PF6-lacI-tetR</i> ( <i>gen</i> ), <i>bgaA::Plac-licB-E170A</i> ( <i>tet</i> )	This study
VL4255	<i>prsI::PF6-lacI-tetR</i> ( <i>gen</i> ), <i>bgaA::Plac-licB-R191A</i> ( <i>tet</i> )	This study
VL4256	<i>prsI::PF6-lacI-tetR</i> ( <i>gen</i> ), <i>bgaA::Plac-licB-H43A</i> ( <i>tet</i> )	This study
Oligo	Sequence	Reference
R191A_for	GAAGCCCTCTTAATCGCTCAAGTAACCTCG	This study
R191A_rev	CGAAGTTACTGAGCGATTAAGAGGGCTTC	This study
H43A_for	GTGGCTGCAACTGCTGATTITTGAGCATC	This study
H43A_rev	GATGCTCAAAAATCAGCAGTTGCAGCCAC	This study
Y233A (gBlock)	GATCCTCAATTGCTAGGGTCTCATGATTGTTTGACGCCCTTGATATGATT TCCTGCGTTGGCTTATTATATCGCTATCAATCGCTTGCACCCAGCCAAGGCT ACAGGCTTGAACCGTGAGCTATGAGCTATGAGTATGGACGGCTTGTGAGTTGTT TTCTTGGGTGCACCGCTAGATATGCTGACCATTATGACGTCACTTGTGCGTC ATTGCTGGAGTTATATTATTAAAGAATAAGGATCCGATCCT	This study
Y236A (gBlock)	GATCCTCAATTGCTAGGGTCTCATGATTGTTTGACGCCCTTGATATGATT TCCTACTTGGCTTATTATATCGCTATCAATCGCTTGCACCCAGCCAAGGCT ACAGGCTTGGCGGTGAGCTATGAGTATGGACGGCTTGTGAGTTGTT TTCTTGGGTGCACCGCTAGATATGCTGACCATTATGACGTCACTTGTGCGTC ATTGCTGGAGTTATATTATTAAAGAATAAGGATCCGATCCT	This study
N252A (gBlock)	GATCCTCAATTGCTAGGGTCTCATGATTGTTTGACGCCCTTGATATGATT TCCTACTTGGCTTATTATATCGCTATCAATCGCTTGCACCCAGCCAAGGCT ACAGGCTTGGCGGTGAGCTATGAGTATGGACGGCTTGTGAGTTGTT TTCTTGGGTGCACCGCTAGATATGCTGACCATTATGACGTCACTTGTGCGTC ATTGCTGGAGTTATATTATTAAAGAATAAGGATCCGATCCT	This study
W17A (gBlock)	GATCCTCATATGAAAAGTAAAAACGGAGTCCCTTGGCCCTCTCAGGT ATTTTCGGGGCTGGCTAACGGTTAGTGCCTATCTTTCGATTITTA CAGATTGTCACCCCTTGTGGCTGCAACTCATGATTITTGAGCATCT TTATCTTACTAGCTTCTTGTGAAAGAAGGGAAAGTTGCGCTCTCAA TTTCTTAAATATCGCAATGTCAGTGTATCATCGGAGCCTGCTAGCGA TCCT	This study
W167A (gBlock)	GATCCTGCTAGCAGGCCCTATCGGTATGCAGGCCAATCTTATGCAGTTA AGTATATCGGAAGTTCTTCTGCTTCTGATCGGTATTTACCCCTGCGA TTTCAGTTCTATTGGCTTCTCTTGAAGCACAAGATTTCGAAAAATA CTGTATTGGGATGTCTGATTATGGAGGGATTATGCTCAGACCTATA AGGGTGAACAGGTTAATTCTTCTACATGGGATTCTTGCTTGGTT GTGCTATTGCGAGGGAAAGTGCAGTGTCTTAGCTTGTGCTTGGTT AGTGAATTGAGTGAATCGAAGCCCTCTAATCCGTCAGTAACCTCGTT CTTGTCTTCTCATCGTGTCTCATCAGTCATTACTGCAGTA GCCAATGGACAATTGGATCCT	This study
E170A (gBlock)	GATCCTGCTAGCAGGCCCTATCGGTATGCAGGCCAATCTTATGCAGTTA AGTATATCGGAAGTTCTTCTGCTTCTGATCGGTATTTACCCCTGCGA TTTCAGTTCTATTGGCTTCTCTTGAAGCACAAGATTTCGAAAAATA CTGTATTGGGATGTCTGATTATGGAGGGATTATGCTCAGACCTATA AGGGTGAACAGGTTAATTCTTCTACATGGGATTCTTGCTTGGTT GTGCTATTGCGAGGGAAAGTGCAGTGTCTTAGCTTGTGCTTGGTT AGTGAATTGAGTGAATCGAAGCCCTCTAATCCGTCAGTAACCTCGTT CTTGTCTTCTCATCGTGTCTCATCAGTCATTACTGCAGTA GCCAATGGACAATTGGATCCT	This study
OVL2077	ATTCCTCTTAACGCCCAAGTC	This study
OVL2082	GTCTCTTTTACCTTGTGCTCTCATCGTGTCTCATCAGTCATTACTGCAGTA GCCAATGGACAATTGGATCCT	This study
OVL5139	TTAATTCCCTCTTAACGCCCAAGT	This study

OVL5623	AGCTGTCGTCGATAGATCCTTCTCCTTTAGATCTTGAAATTGCG GCCG	This study
OVL5624	AGCTGTCGTCGCTATGAAAAGTAAAAACGGAGTTCCCTTGGCCTCTC TCAG	This study
OVL5625	AGCTGTCGTCGCTTATTCTTAATAATAATATAAACTCCAGCAATGACG ACA	This study
OVL5626	AGCTGTCGTCTCGtaaGTCGACCTCGAGACTAGTCAAGGTCGGCAATTCTGC AGTA	This study
OVL5635	AACTCTTCGACAAAATGCGCATCGTCTATCTGAAAATAAC	This study
OVL5636	GAAAATGCTATCCAATGAT	This study
OVL6035	TAAGGGCGTCTCGCGAAATCATATCAAAGGCTGAAAAA	This study
OVL6036	TAAGGGCGTCTCCCGCATTGGCTTATTATATCGCTATCA	This study
OVL6037	AGTGGTCGTCCTCGCAGCCAAGTAGGAATCATATCAAAGGCTGAAAAA ACAATC	This study
OVL6038	AGTGGTCGTCCTCGCTGCATATATCGCTATCAATCGCTTGCACCAGCAA GGCTA	This study
OVL6039	GGAATGCGTCTCGCGAAAATACCTGAGAGAAGGCCAAAGGAAC	This study
OVL6040	GGAATGCGTCTCGTCGCAGGCTTGGGTCTAACGGTTAGTGCTTAT	This study
OVL6041	GCCATACGTCTCGGCTGCAATAGCACAAACCAAAGCACAGAGAAT	This study
OVL6042	GCCATACGTCTCCCAGCAGGAAGTGAGAGTGTTAGCTCCTT	This study
OVL6043	CATCCACGTCTCGGCACTTCCCCATGCAATAGCACAAACCAAAGC	This study
OVL6044	CATCCACGTCTCGTGCAGTGTTAGCTCCTTGCTATGGAA	This study
OVL6045	GACAACCGTCTCGCGATTAAGAGGGCTCGATTCACTCAGTT	This study
OVL6046	GACAACCGTCTCCCGCACAAGTGACTTCGTTGTCTTATCTT	This study
OVL6047	CTCCTACGTCTCCCGCAGTTGCAGGCCACCAAAAGGGTGACAAATC	This study
OVL6048	CTCCTACGTCTCCCTGCAGATTTTGAGCATCTTATCTTACTA	This study